Time-Domain Selected Mapping with Polyphase Rotations and Blind Detection for Filtered Single-Carrier Signals

Amnart Boonkajay[†]　　and Fumiyuki Adachi[‡]

[†][‡]Department of Communications Engineering, Graduate School of Engineering, Tohoku University

6-6-05 Aza-Aoba, Aramaki, Aoba-ku, Sendai, Miyagi, 980-8579 Japan

E-mail:　[†]amnart@mobile.ecei.tohoku.ac.jp　　[‡]adachi@ecei.tohoku.ac.jp

Abstract　Single-carrier (SC) signal has a low peak-to-average power ratio (PAPR) property. However, the PAPR of filtered SC signal increases if high-level modulation is applied. We have recently proposed a time-domain selected mapping (TD-SLM) which effectively reduces the PAPR of filtered SC signals by applying the binary phase rotation before transmit filtering, but the necessity of side-information decreases the spectrum efficiency (SE). In this paper, a TD-SLM with maximum likelihood (ML) joint blind identification of phase rotation pattern and data detection (hereafter joint blind identification and detection) is introduced. Unlike the frequency-domain SLM (FD-SLM), polyphase rotations are used in order to allow the blind detection. Performance evaluation of the proposed TD-SLM with joint blind identification and detection is done by computer simulation assuming uncoded filtered SC block signal transmission in aspects of PAPR, bit-error rate (BER) and throughput to show that no significant degradation is caused in the BER performance.

Keyword　Single-carrier (SC) transmission, peak-to-average power ratio (PAPR), selective mapping (SLM), frequency-domain equalization (FDE)

1. Introduction

Single-carrier (SC) transmission with frequency-domain equalization (FDE) [1] is a robust transmission technique in a frequency-selective fading channel [2], while its transmit waveform has low peak-to-average power ratio (PAPR) [3]. Transmit filtering is typically applied to SC-FDE for band-limiting the transmit signal, but the use of transmit filtering increases the PAPR of SC-FDE [4], [5]. Therefore, PAPR reduction of filtered SC-FDE signal remains an important issue. A PAPR reduction technique based on phase rotation called selected mapping (SLM) is very attractive since it is a distortionless technique providing effective PAPR reduction [6].

We have recently proposed SLM-based PAPR reduction techniques for SC-FDE, where the phase rotation is applied either in frequency domain or time domain [7], [8]. In frequency-domain based SLM (FD-SLM) [7], the phase rotation is applied between discrete Fourier transform (DFT) and inverse DFT (IDFT). In time-domain based SLM (TD-SLM) [8], the phase rotation is applied directly to data-modulated transmit block before transmit filtering. It is shown in [7], [8] that both SLM techniques can effectively reduce the PAPR of filtered SC-FDE. TD-SLM better reduces the PAPR than FD-SLM for the same number of phase rotation pattern candidates. BER performance can be preserved as the same as conventional SC-FDE, but transmitting side-information is required [9].

Blind signal detection based on maximum likelihood (ML) [10] provides good detection performance without sending side-information. Its complexity can be further reduced by using shared phase-rotation codebook for limiting the number of phase rotation pattern candidates. The ML blind detection with shared phase-rotation codebook was proposed for orthogonal frequency division multiplexing (OFDM) with SLM [11] and SC-FDE using FD-SLM [12], where those blind detection schemes achieve similar BER to that with ideal side-information sharing. However, the blind detection for SC-FDE using TD-SLM is still undetermined; in addition, the blind detection in [11], [12] cannot be applied straightforwardly to TD-SLM.

In this paper, the joint blind identification of phase rotation patterns and data detection (hereinafter joint blind identification and detection) for SC-FDE using TD-SLM is our main focus. We firstly describe the reasons showing that the proposed blind detection in [11], [12] cannot be used directly. Then we introduce the TD-SLM technique with ML blind detection for SC-FDE. Unlike the blind detection in FD-SLM, de-mapping and Euclidean distance calculation are both carried out in time domain. Polyphase rotations are implemented in TD-SLM instead of binary phase rotation in order to allow the blind detection. Performance evaluation of proposed blind detection is done by computer simulation in terms of PAPR, BER and throughput.

The rest of this paper is organized as follows. Section 2 introduces the TD-SLM algorithm with polyphase rotations. Section 3 shows the transmitter model of SC-FDE using TD-SLM. Section 4 shows the receiver model with joint blind identification and detection. Section 5 provides simulation performances, and Section 6 concludes the paper.
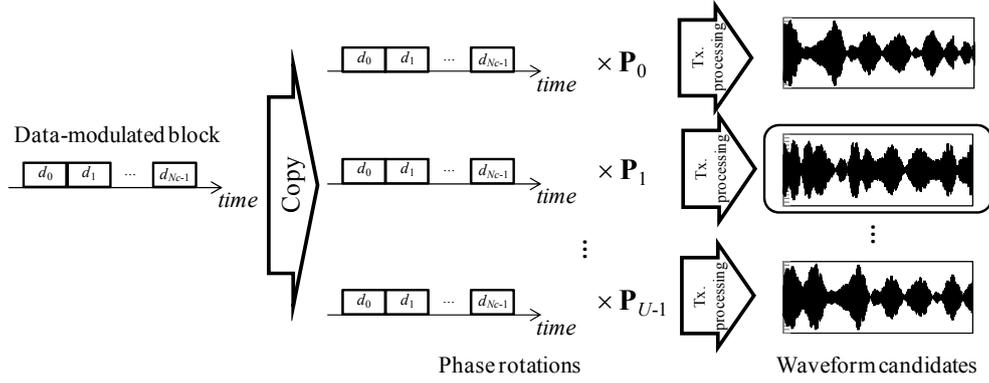
Fig.1 TD-SLM algorithm.

2. TD-SLM algorithm

Assuming that an N_c-length time-domain transmit block is represented by a vector $\mathbf{s}=[s(0),s(1),\ldots,s(N_c-1)]^T$, PAPR of the time-domain transmit signal calculated over an oversampled transmission block is expressed by

$$\text{PAPR}(\mathbf{s})=\frac{\max\left\{|s(n)|^2, n=0,\frac{1}{V},\frac{2}{V},\ldots,N_c-1\right\}}{E[|s(n)|^2]}, \qquad (1)$$

where V is oversampling factor. TD-SLM algorithm considered in this paper is similar to the algorithm in [8], where its signal processing is illustrated by Fig. 1.

A set of U different $N_c \times N_c$ diagonal matrices representing phase rotation $\mathbf{P}_u=diag[P_u(0),\ldots,P_u(N_c-1)]$, $u=0 \sim U-1$ is defined. $\mathbf{P}_u$ is multiplied to time-domain data-modulated transmit block $\mathbf{d}=[d(0),\ldots,d(N_c-1)]^T$, which is different from FD-SLM in [6], [7], then obtaining the time-domain transmit candidate $\mathbf{d}_u=\mathbf{P}_u\mathbf{d}$. In [8], the phase rotation pattern candidates are set to be $P_u(n)=\pm1$, $n=0 \sim N_c-1$ and are generated from 4095-bit pseudonoise sequence, except the phase rotation matrix for the first pattern is set to be an $N_c \times N_c$ identity matrix $\mathbf{I}_{N_c}$ as a representative of original transmit block. However, the use of binary phase rotation causes false detection when the joint blind identification and detection is applied at the receiver, and hence the polyphase rotations should be applied instead. In this paper, we use the polyphase rotation pattern candidates which are randomly generated as $P_u(n)\in\{e^{j0}, e^{j(2\pi/3)}, e^{-j(2\pi/3)}\}$, $n=0 \sim N_c-1$, $u=1 \sim U-1$. The details about phase rotation pattern design are discussed in Section 4.

All time-domain transmit candidates $\mathbf{d}_u$ are then passed through transmit signal processing (the details are described in Section 3). The instantaneous PAPR of time-domain transmit signal after processing $\mathbf{s}_u=[s_u(0),\ldots,s_u(N_c-1)]^T$ are calculated by referring (1), and the selected transmit signal $\mathbf{s}_{\hat{u}}=[s_{\hat{u}}(0),\ldots,s_{\hat{u}}(N_c-1)]^T$ with the corresponding selected phase rotation pattern index $\hat{u}$ is selected by the following criterion

$$\hat{u}=\arg\min_{u=0,1,\ldots,U-1}\text{PAPR}(\mathbf{s}_u=\mathbf{F}_{N_c}^H\mathbf{H}_T\mathbf{F}_{N_c}\mathbf{P}_u\mathbf{d}). \qquad (2)$$
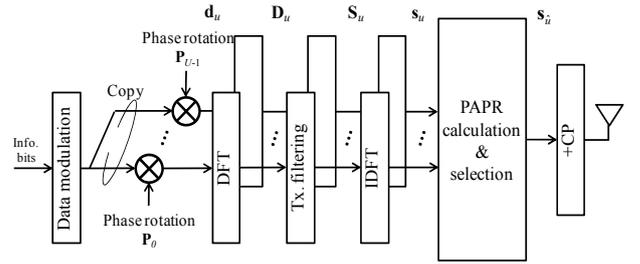
(a) Transmitter
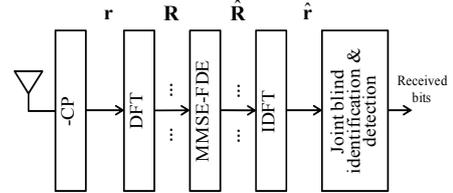
(b) Receiver

Fig.2 Transmission models of filtered SC-FDE with blind TD-SLM.

Note that the matrix and vector representations for transmit signal processing in (2) are described in more details in Section 3.

3. SC-FDE Transmitter with TD-SLM

Single-user N_c-length block transmission with N_g-length of cyclic prefix (CP) insertion is assumed. DFT and IDFT are employed for reaching frequency-domain processing, at which the transmit filtering can be simply done as one-tap multiplication. Transmitter model of filtered SC-FDE equipped with TD-SLM is illustrated by Fig. 2(a).

A transmit block consisting of N_c data-modulated symbols $\mathbf{d}=[d(0),\ldots,d(N_c-1)]^T$ is used for generating U transmit block candidates for TD-SLM $\mathbf{d}_u$ by applying different phase rotation patterns. The u-th transmit block candidate is expressed by

$$\mathbf{d}_u=\mathbf{P}_u\mathbf{d}, \qquad (3)$$

where $\mathbf{P}_u$ represents phase rotation matrix and the generation of $P_u(n)$ is already discussed in Section 2. Next, each transmit block candidate is transformed into

frequency domain, yielding frequency-domain transmit signal of the u-th candidate $\mathbf{D}_u=[D_u(0),...,D_u(N_c-1)]^T$ as

$$\mathbf{D}_u = \mathbf{F}_{N_c}\mathbf{P}_u\mathbf{d}, \tag{4}$$

where the N_c-point DFT matrix $\mathbf{F}_{N_c}$ is expressed by

$$\mathbf{F}_{N_c} = \frac{1}{\sqrt{N_c}}\begin{bmatrix} 1 & 1 & \cdots & 1 \\ 1 & e^{\frac{-j2\pi(1)(1)}{N_c}} & \cdots & e^{\frac{-j2\pi(1)(N_c-1)}{N_c}} \\ \vdots & \vdots & \ddots & \vdots \\ 1 & e^{\frac{-j2\pi(N_c-1)(1)}{N_c}} & \cdots & e^{\frac{-j2\pi(N_c-1)(N_c-1)}{N_c}} \end{bmatrix}, \tag{5}$$

and its Hermitian transpose represents IDFT operation.

Next, $\mathbf{D}_u$ is multiplied by the transmit filtering matrix $\mathbf{H}_T=diag[H_T(0),...,H_T(N_c-1)]$, yielding frequency-domain filtered signal $\mathbf{S}_u=\mathbf{H}_T\mathbf{D}_u$. Note that we apply the transmit filtering in frequency domain instead of in time domain since it can be applied as one-tap multiplication, which requires lower complexity compared to convolution. In addition, SRRC filter with roll-off factor $\alpha=0$ (i.e. ideal rectangular filter) is assumed for the transmit filtering.

After that, $\mathbf{S}_u$ is transformed back into time domain by N_c-point IDFT matrix $\mathbf{F}_{N_c}^H$. PAPR calculation is applied in order to search and selected the time-domain transmit signal with the lowest PAPR based on (2). The selected transmit signal based on TD-SLM is expressed by

$$\mathbf{s}_{\hat{u}} = \mathbf{F}_{N_c}^H\mathbf{H}_T\mathbf{F}_{N_c}\mathbf{d}_{\hat{u}} = \mathbf{F}_{N_c}^H\mathbf{H}_T\mathbf{F}_{N_c}\mathbf{P}_{\hat{u}}\mathbf{d}. \tag{6}$$

Finally, the last N_g samples of transmit block are copied as CP and inserted into the guard interval (GI), then a CP-inserted signal block of N_g+N_c samples is transmitted.

4. Receiver with Blind Detection

Received signal representation and blind detection algorithm without side-information are described in this section. The ML blind detection has been proposed for OFDM [11] and SC-FDE with FD-SLM [12], however, the proposed blind detection in [11], [12] cannot be used straightforwardly in TD-SLM. The modification for allowing blind detection in TD-SLM is also introduced in this section.

4.1 Received Signal Representation

Receiver block diagram is illustrated by Fig. 2(b). The propagation channel is assumed to be a symbol-space L-path frequency-selective block fading channel [2], where its impulse response between transmitter and receiver is

$$h(\tau) = \sum_{l=0}^{L-1} h_l\delta(\tau-\tau_l), \tag{7}$$

where h_l and τ_l are complex-valued path gain and time delay of the l-th path, respectively. $\delta(\cdot)$ is the delta function. Time-domain signal vector after CP removal $\mathbf{r}=[r(0),...,r(N_c-1)]^T$ is expressed by

$$\mathbf{r} = \sqrt{\frac{2E_s}{T_s}}\mathbf{hs}_{\hat{u}} + \mathbf{n}, \tag{8}$$

where $\mathbf{s}_{\hat{u}} = \mathbf{F}_{N_c}^H\mathbf{H}_T\mathbf{F}_{N_c}\mathbf{P}_{\hat{u}}\mathbf{d}$ is obtained from (6), and $\mathbf{n}$ is noise vector in which element is zero-mean additive white Gaussian noise (AWGN) having the variance $2N_0/T_s$ with T_s is symbol duration and N_0 being the one-sided noise power spectrum density. Channel response matrix $\mathbf{h}$ is a circular matrix representing time-domain channel response, which is

$$\mathbf{h} = \begin{bmatrix} h_0 & & h_{L-1} & \cdots & h_1 \\ h_1 & \ddots & & \ddots & \vdots \\ \vdots & h_0 & \mathbf{0} & & h_{L-1} \\ h_{L-1} & h_1 & \ddots & & \\ & \ddots & \vdots & & \ddots \\ \mathbf{0} & h_{L-1} & \cdots & \cdots & h_0 \end{bmatrix}. \tag{9}$$

The received signal vector $\mathbf{r}_{\hat{u}}$ is transformed into frequency domain by N_c-point DFT, obtaining the frequency-domain received signal $\mathbf{R}$ as

$$\begin{aligned} \mathbf{R} &= \sqrt{\frac{2E_s}{T_s}}\mathbf{F}_{N_c}\mathbf{hs}_{\hat{u}} + \mathbf{F}_{N_c}\mathbf{n} \\ &= \sqrt{\frac{2E_s}{T_s}}\mathbf{F}_{N_c}\mathbf{hF}_{N_c}^H\mathbf{H}_T\mathbf{F}_{N_c}\mathbf{P}_{\hat{u}}\mathbf{d} + \mathbf{F}_{N_c}\mathbf{n}, \\ &= \sqrt{\frac{2E_s}{T_s}}\mathbf{H}_c\mathbf{H}_T\mathbf{F}_{N_c}\mathbf{P}_{\hat{u}}\mathbf{d} + \mathbf{N} \end{aligned} \tag{10}$$

where the frequency-domain channel response $\mathbf{H}_c$ is defined as $\mathbf{F}_{N_c}\mathbf{hF}_{N_c}^H = diag[H_c(0),...,H_c(N_c-1)] \equiv \mathbf{H}_c$.

FDE based on minimum mean-square error criterion (MMSE-FDE) [1] is applied by multiplying the FDE matrix $\mathbf{W}_R=diag[W_R(0),...,W_R(N_c-1)]$ to $\mathbf{R}$, yielding the equalized signal $\hat{\mathbf{R}} = \mathbf{W}_R\mathbf{R}$. The FDE weight at subcarrier k, $W_R(k)$, is derived so as to minimize the MSE between frequency-domain transmit vector $\mathbf{S}_{\hat{u}}$ and $\mathbf{R}$, and is expressed by

$$W_R(k) = \frac{H_c^*(k)H_T^*(k)}{|H_c(k)H_T(k)|^2 + (E_s/N_0)^{-1}}, \tag{11}$$

where $H_c(k)$ is the k-th element in the diagonal of $\mathbf{H}_c$, which corresponds to the frequency-domain channel gain at the k-th subcarrier. Note that $W_R(k)$ is independent from phase rotation pattern.

The equalized signal is then transformed into time domain by N_c-point IDFT, yielding time-domain equalized signal vector before de-mapping $\hat{\mathbf{r}}=[\hat{r}(0),...,\hat{r}(N_c-1)]^T$ as

$$\hat{\mathbf{r}} = \mathbf{F}_{N_c}^H\hat{\mathbf{R}} = \sqrt{\frac{2E_s}{T_s}}\mathbf{F}_{N_c}^H\widetilde{\mathbf{H}}_c\mathbf{F}_{N_c}\mathbf{P}_{\hat{u}}\mathbf{d} + \mathbf{F}_{N_c}^H\mathbf{W}_R\mathbf{F}_{N_c}\mathbf{n}, \tag{12}$$

where $\widetilde{\mathbf{H}}_c = \mathbf{W}_R\mathbf{H}_c\mathbf{H}_T$ is the frequency-domain equivalent channel gain. The time-domain equalized signal at time index n, $\hat{r}(n)$, can be expressed by

$$\hat{r}(n) = \sqrt{\frac{2E_s}{T_s}}\left(\frac{1}{N_c}\sum_{k=0}^{N_c-1}\widetilde{H}_c(k)\right)P_{\hat{u}}(n)d(n)$$
$$+\sqrt{\frac{2E_s}{T_s}}\left(\frac{1}{N_c}\sum_{k=0}^{N_c-1}\widetilde{H}_c(k)\sum_{\substack{n'=0\\n'\neq n}}^{N_c-1}P_{\hat{u}}(n')d(n')e^{j2\pi\frac{n-n'}{N_c}}\right), \quad (13)$$
$$+\widetilde{n}(n)$$

where $\widetilde{n}(n)$ is the n-th element in $\widetilde{\mathbf{n}}=\mathbf{F}_{N_c}^H\mathbf{W}_R\mathbf{F}_{N_c}\mathbf{n}$. It is seen that the first term in (13) represents the desired signal, where the second term and the third term are residual ISI and noise, respectively.

In general, time-domain received vector before de-modulation $\hat{\mathbf{d}}=[\hat{d}(0),...,\hat{d}(N_c-1)]^T$ is obtained by applying de-mapping [8], which can be simply done by multiplying the Hermitian transpose of selected phase rotation matrix, i.e. $\hat{\mathbf{d}}=\mathbf{P}_{\hat{u}}^H\hat{\mathbf{r}}$. However, side-information transmission is required to let the receiver know the information of $\mathbf{P}_{\hat{u}}$. A signal detection for TD-SLM without information of $\mathbf{P}_{\hat{u}}$, i.e. blind detection, is introduced in the next subsection.

4.2 Blind Detection Algorithm

The joint blind identification and detection has been proposed for OFDM [11] and SC-FDE using FD-SLM [12]. In [12], received candidate generation is done in frequency domain, where the MSE calculation (which is equivalent to square Euclidean distance calculation) is done in time domain after IDFT. In [11], candidate generation and MSE calculation are both done in frequency domain. The blind detection described in this subsection is partially similar to that of [11], however, both candidate generation and MSE calculation are carried out in time domain instead. Note that the effect of residual ISI is not considered in [11].

The ML blind detection is used to estimate the time-domain received symbols $\widetilde{\mathbf{d}}=[\widetilde{d}(0),...,\widetilde{d}(N_c-1)]^T$ with the corresponding selected phase rotation matrix $\mathbf{P}_v$. Received symbols vector estimation is selected as the candidate providing the lowest MSE from $\hat{\mathbf{r}}$, and the selection criterion can be expressed by the following equation.

$$\widetilde{\mathbf{d}}=\min_{\substack{P_v(n)\in\Phi_{\text{SLM}}\\\widetilde{d}(n)\in\Psi_{\text{mod}}}}\frac{1}{N_c}\sum_{n=0}^{N_c-1}\left|\hat{r}(n)P_v^*(n)-\widetilde{d}(n)\right|^2, \quad (14)$$

where Φ_{SLM} is a set of possible phase rotation, which is assumed to be $\Phi_{\text{SLM}}=\{e^{j0},e^{j(2\pi/3)},e^{-j(2\pi/3)}\}$ in this paper. Ψ_{mod} is a set of constellations for each modulation level, for example, $\Psi_{\text{mod}}=\{\frac{3}{\sqrt{10}}+j\frac{3}{\sqrt{10}},\frac{3}{\sqrt{10}}+j\frac{1}{\sqrt{10}},...,-\frac{3}{\sqrt{10}}-j\frac{3}{\sqrt{10}}\}$ in case of 16-QAM.

However, the blind detection in (14) requires very high computational complexity. The complexity can be simply reduced by using fixed set of phase rotation patterns, i.e. the set is once randomly generated and then is used for every transmission time. By using the fixed set and shared codebook between transceiver, (14) can be re-written as
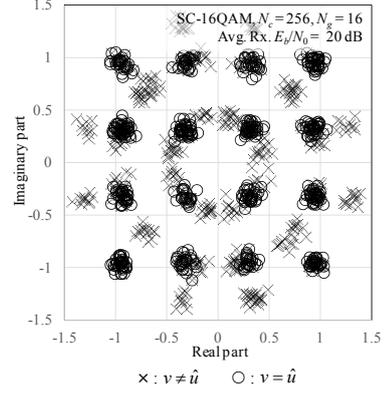

Fig.3 One-shot observation of received signal vector $\mathbf{P}_v^H\hat{\mathbf{r}}$.

$$\widetilde{\mathbf{d}}=\min_{\substack{\mathbf{P}_v,v=0,1,...,U-1\\\widetilde{d}(n)\in\Psi_{\text{mod}}}}\frac{1}{N_c}\sum_{n=0}^{N_c-1}\left|\hat{r}(n)P_v^*(n)-\widetilde{d}(n)\right|^2. \quad (15)$$

The joint blind identification and detection in (15) can reduce the number of complex-valued multiplication from $3^{N_c}\times N_c\times N_{\text{mod}}^2$ to $U\times N_c\times(N_{\text{mod}}^2+1)$, where N_{mod} represents modulation level (2 for 4QAM, 4 for 16QAM and 6 for 64QAM). It is also described in [11] by assuming OFDM transmission that the blind detection in (15) needs to meet the following criterions:

- The set of phase rotation patterns $\{\mathbf{P}_u, u=0\sim U-1\}$ is fixed for every transmit block and is known *a priori*.
- $c(n)P_u(n)\notin\Psi_{\text{mod}}$ for all $n=0\sim N_c-1$, $u=0\sim U-1$ and for a given $\mathbf{c}=[c(0),...,c(N_c-1)]^T$ and $c(n)\in\Psi_{\text{mod}}$. This criterion implies that the binary phase rotation $(P_u(n)=\pm1)$ cannot be used.

The first criterion is cleared by using a shared codebook. Even though the second criterion can be exempted in the blind detection for FD-SLM since de-mapping and MSE calculation are carried out in different domain, it needs to be accomplished in TD-SLM similar to that of OFDM transmission.

It is known from [13] and [14] that the phase rotation should be randomized and uniformly distributed in $[0,2\pi)$. However, phase rotation distribution with the interval of $2\pi/A$ when A is even number (e.g. if $A=4$, $P_u(n)\in\{e^{j0},e^{j(2\pi/4)},e^{j(4\pi/4)},e^{j(6\pi/4)}\}$) cannot be used since the criterion of $c(n)P_u(n)\notin\Psi_{\text{mod}}$ is not met when the SC-FDE transmission with TD-SLM is considered. On the other hand, $c(n)P_u(n)\notin\Psi_{\text{mod}}$ is accomplished when A is odd number, and hence the discrete, uniformly-distributed phase rotation $P_u(n)\in\{e^{j0},e^{j(2\pi/3)},e^{-j(2\pi/3)}\}$ (i.e. $A=3$) is selected to be used in the TD-SLM in this paper.

In addition, Fig. 3 shows one-shot observation of $\mathbf{P}_v^H\hat{\mathbf{r}}$ assuming SC-FDE with 16-QAM modulation at average received bit energy-to-noise power spectrum density ratio E_b/N_0=20 dB, where E_b/N_0=$(1/N_{\text{mod}})(E_s/N_0)(N_c/(N_c+N_g))$. It is seen that $\mathbf{P}_v^H\hat{\mathbf{r}}$ is very close to the original 16QAM signal constellations when $v=\hat{u}$, while most samples in $\mathbf{P}_v^H\hat{\mathbf{r}}$ are slightly split from the original constellations when $v\neq\hat{u}$. This also implies that the blind detection in (15) has a potential to achieve high-accuracy detection when the received power is sufficiently high.
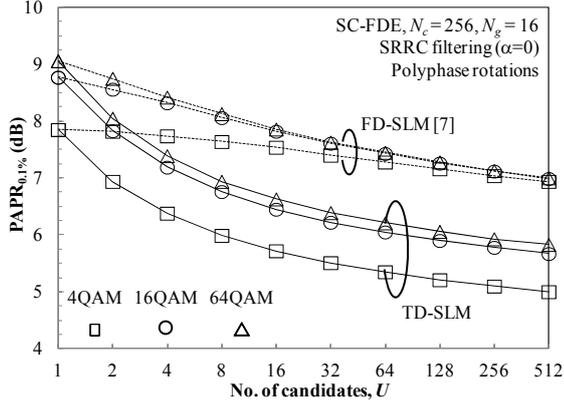
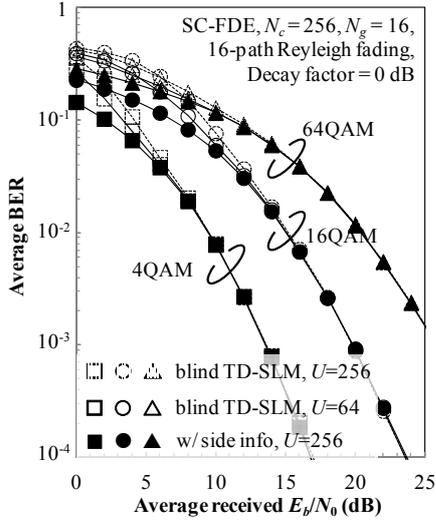**Fig.4** $PAPR_{0.1\%}$ versus the number of candidates.

Fig. 5 BER performances.

Table 1 Simulation parameters.

Transmitter	Data modulation	4QAM, 16QAM, 64QAM
	FFT block size	$N_c = 256$
	CP length	$N_g = 16$
SLM parameters	Phase rotation	Polyphase ($0°$, $\pm120°$)
	# of candidates	$U = 1$(no SLM)~512
Channel	Fading	Frequency-selective block Rayleigh
	Power delay profile	Symbol-spaced, 16-path uniform
Receiver	Channel estimation	Ideal
	Side-information detection	TD-SLM $\rightarrow$ Ideal
	FDE	MMSE-FDE

5. Performance Evaluation

Numerical and simulation parameters are summarized in Table 1. We assume SC-FDE block transmission with the number of available subcarriers N_c=256. Oversampling factor is set to be V=8. System performances of the conventional SC-FDE, SC-FDE using TD-SLM (with side-information) and SC-FDE with blind TD-SLM are evaluated in terms of PAPR, BER and throughput.

5.1 PAPR

PAPR performance is evaluated by measuring the PAPR value at complementary cumulative distribution function (CCDF) equals 10^{-3}, called $PAPR_{0.1\%}$, where its definition is $prob(PAPR(\mathbf{s}) \geq PAPR_{0.1\%}) = 10^{-3}$.

Fig 4 shows the $PAPR_{0.1\%}$ of SC-FDE using blind TD-SLM and conventional FD-SLM as a function of number of phase rotation pattern candidates (U). The performance of SC-FDE using FD-SLM is evaluated by referring [7]. The $PAPR_{0.1\%}$ of conventional SC-FDE is shown at the place with U=0. It is seen that $PAPR_{0.1\%}$ decreases when U increases in both SLM approaches because of an increasing of degree of freedom, which results in higher probability to obtain the transmit waveform with lower PAPR among the candidates. SC-FDE using blind TD-SLM also achieves lower $PAPR_{0.1\%}$ compared to FD-SLM in every U. The reason is already discussed in [8] as generating transmit block candidates in time domain directly transforms the "bad" arrangement of data-modulated symbols to another arrangement which possibly has lower PAPR [15]. In addition, $PAPR_{0.1\%}$ of blind TD-SLM in Fig. 4 is same as in [8] even though the polyphase rotations are applied instead of binary phase rotation.

5.2 BER performance

Fig. 5 shows the BER as a function of average received E_b/N_0 of SC-FDE using blind TD-SLM. BER performance of TD-SLM with ideal side-information detection at U=256 is also shown for comparison. Channel coding is not considered in this paper. It can be seen that BER performances degrade when U increases at low received E_b/N_0 region. The above result can be described by referring Eqs. (13) and (15) and Section 4.2, as the effect from noise enhancement and residual ISI causes difficulty in phase rotation pattern estimation since the residual ISI and noise make $\mathbf{P}_v^H \hat{\mathbf{r}}$ become apart from original constellations even though $v = \hat{u}$.

However, the BER performance of blind TD-SLM becomes similar to that of TD-SLM with ideal side-information detection when $E_b/N_0 \geq 8$ dB for 4QAM and 64QAM, and $E_b/N_0 \geq 12$ dB for 16QAM. The above results conclude that the proposed SC-FDE with blind TD-SLM and polyphase rotation can be used effectively when E_b/N_0 is sufficiently high.

5.3 Throughput Performance

Throughput performance of SC-FDE using blind TD-SLM is evaluated as a function of peak transmit E_s/N_0, where the throughput (η) in bps/Hz is defined by [4]

$$\eta = N_{mod} \times (1-PER) \times \frac{1}{1+\alpha} \times \frac{1}{1+\frac{N_g+N_{SI}}{N_c}}, \quad (16)$$

where PER is packet-error rate and $N_{SI} = \lceil (\log_2 U)/N_{mod} \rceil$ is the number of required side-information symbols. Peak

transmit E_s/N_0 is defined as a summation of average received E_s/N_0 and $PAPR_{0.1\%}$, and is considered since it refers to the required peak transmit power of a power amplifier (PA) [4].

Fig. 6 shows the average throughput of performances of conventional SC-FDE, SC-FDE using TD-SLM (with ideal side-information sharing) and SC-FDE using blind TD-SLM. Channel coding and packet retransmission are not considered in this paper. TD-SLM is set to achieve $PAPR_{0.1\%} \le 6$ dB, i.e. U equals 8 for 4QAM, 128 for 16QAM and 256 for 64QAM. SC-FDE using TD-SLM with ideal side-information detection provides better throughput at low peak E_s/N_0 region compared to the SC-FDE without SLM because of lower PAPR, but the peak throughput slightly degrades. On the other hand, there is no degradation of peak throughput when the blind TD-SLM is applied, while the improvement of throughput at low peak E_s/N_0 region is achieved similar to TD-SLM with side-information.

6. Conclusion

In this paper, TD-SLM with polyphase rotations and blind detection for filtered SC-FDE was proposed. The joint blind identification and detection is carried out by calculating the MSE of the received block candidates generated from a set of phase rotation patterns. We also introduced the design criteria for polyphase rotations and the corresponding phase rotation patterns in order to allow the blind detection. Simulation results confirmed that filtered SC-FDE transmission using the proposed blind TD-SLM achieves low-PAPR transmission without degradation on throughput performance.

References

[1] D. Falconer, S. L. Ariyavisitakul, A. Benyamin-Seeyar and B. Edison, "Frequency Domain Equalization for Single-Carrier Broadband Wireless Systems," *IEEE Commun. Mag.*, Vol. 40, No. 4, pp. 58-66, Apr. 2002.

[2] A. Goldsmith, *Wireless Communications*, Cambridge University Press, 2005.

[3] H. Sari, G. Karam and I. Jeanclaude, "Transmission Techniques for Digital Terrestrial TV Broadcasting," *IEEE Commun. Mag.*, Vol. 33, No. 2, pp. 100-109, Feb. 1995.

[4] S. Okuyama, K. Takeda and F. Adachi, "MMSE Frequency-domain Equalization using Spectrum Combining for Nyquist Filtered Broadband Single-Carrier Transmission," *in Proc. IEEE Veh. Technol. Conference (VTC 2010-Spring)*, Taipei, Taiwan, May 2010.

[5] A. Boonkajay, T. Obara, T. Yamamoto and F. Adachi, "Excess-Bandwidth Transmit Filtering Based on Minimization of Variance of Instantaneous Transmit Power for Low-PAPR SC-FDE," *IEICE Trans. Commun.*, Vol. E98-B, No. 4, pp. 673-685, Apr. 2015.

[6] R. W. Bauml, R. F. H. Fischer and J. B. Huber, "Reducing the Peak-to-Average Power Ratio of Multicarrier Modulation by Selected Mapping," *IEEE Electron. Lett.*, Vol. 32, No. 22, pp. 2056-2057, Oct. 1996.

[7] A. Boonkajay, T. Obara, T. Yamamoto and F. Adachi, "Selective Mapping for Broadband Single-Carrier Transmission Using Joint Tx/Rx MMSE-FDE," *in Proc.*

IEEE Int. Symp. On Personal Indoor and Mobile Radio Commun. (PIMRC 2013), London, U.K., Sept. 2013.

[8] A. Boonkajay and F. Adachi, "Low-PAPR Joint Transmit/Received SC-FDE Transmission using Time-Domain Selected Mapping," *in Proc. Asia-Pacific Conference on Commun. (APCC 2014)*, Pattaya, Thailand, Oct. 2014.

[9] S. S. Eom, H. W. Nam and Y. C. Ko, "Low-Complexity PAPR Reduction Scheme Without Side Information for OFDM Systems," *IEEE Trans. Signal Process.*, Vol. 60, No. 7, pp. 3657-3669, Jul. 2012.

[10] J. G. Proakis and M. Salehi, *Digital Communications*, 5th ed., McGraw-Hill, 2008.

[11] A. D. S. Jayalath and C. Tellambura, "SLM and PTS Peak Power Reduction of ODFM Signal without Side Information," *IEEE Trans. Wireless Commun.*, Vol. 4, No. 5, pp. 2006-2013, Sept. 2005.

[12] A. Boonkajay and F. Adachi, "A Blind Selected Mapping Technique for Low-PAPR Single-Carrier Signal Transmission," *submitted to Int. Conference on Inform. Commun. and Signal Process.*, 2015.

[13] G. T. Zhou and L. Peng, "Optimality Condition for Selected Mapping in OFDM," *IEEE Trans. Signal Process.*, Vol. 54, No. 8, pp. 3159-3165, Aug. 2006.

[14] N. Ohkubo and T. Ohtsuki, "Design Criteria for Phase Sequences in Selected Mapping," *IEICE Trans. Commun.*, Vol. E86-B, No. 9, pp. 2628-2636, Sept. 2003.

[15] V. K. N. Lau, "Average of Peak-to-Average Ratio (PAR) of IS95 and CDMA2000 Systems – Single Carrier," *IEEE Commun. Lett.*, Vol. 5, No. 4, pp. 160-162, Apr. 2001.
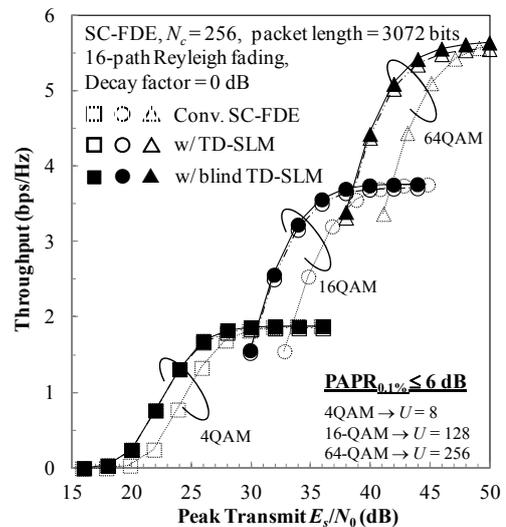
Fig.6 Throughput performances.